

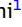




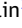



RESEARCH REPORT

Blocking nitric oxide production for glioblastoma: A targeted therapeutic approach

Shashank Kumar Ojha¹ , Wisam Bazbaz¹ , Manish Kumar Tripathi¹ , Maryam Kartawy¹ , Shelly Ginzburg¹ , Anna Mouraviov¹, Mallikarjuna Nimgampalle¹ , Wajeha Hamoudi¹ , Igor Khaliulin¹ , and Haitham Amal^{1,2,3} 

¹Institute for Drug Research, School of Pharmacy, Faculty of Medicine, The Hebrew University of Jerusalem, Ein Karem, Jerusalem 9112102, Israel

²Rosamund Stone Zander Translational Neuroscience Center, Boston Children's Hospital, Boston, MA 02115, USA

³Department of Neurology, Boston Children's Hospital, Harvard Medical School, Boston, MA 02115, USA

Corresponding Author: Haitham Amal, Rosamund Stone Zander Translational Neuroscience Center, Boston Children's Hospital, Boston, MA 02115, USA. E-mail: Haitham.amal@mail.huji.ac.il, Haitham.amal85@gmail.com

Brain Medicine; <https://doi.org/10.61373/bm025r.0050>

Glioblastoma (GBM) represents the foremost prevalent and aggressive form of primary brain tumor, characterized by high morbidity and mortality rates. Nitric oxide (NO) has been shown to have diverse effects on various cancers, including GBM. Our previous study has shown NO synthase (NOS) hyperactivation in GBM cell lines. GBM cell survival was reversed by the NOS-targeting pharmacological inhibition in vitro. The current work explores the impact of inducible and neuronal NOS (iNOS and nNOS) inhibitors, BA-103 and BA-101, respectively, on a glioblastoma xenograft model. Both agents mitigate nitrosative stress through distinct mechanisms. NOD-SCID mice were used to establish a subcutaneous xenograft tumor model with U-87 MG cells. BA-103 and BA-101 were administered to mice via intraperitoneal injections. Tumor metrics, including weight and volume, were assessed. Immunofluorescence and Western blots were conducted to assess nitrosative stress, tumor proliferation, and cell death. Treatment with the NOS inhibitors, particularly with BA-101, significantly reduced tumor volume in the xenograft model. A dose-dependent study with BA-101 identified 80 mg/kg as the most efficacious dose for GBM treatment. Combining BA-101 with the antitumor drug temozolomide (TMZ) synergistically reduced tumor size and significantly increased survivability in mice bearing TMZ-sensitive cells. Our findings suggest that targeting nNOS holds promise as a therapeutic strategy for GBM treatment.

Keywords: Apoptosis, brain, glioblastoma, iNOS, neuroscience, nitric oxide, nNOS.

Introduction

Glioblastoma (GBM) is the most malignant type of glioma (1). GBM is attributed to 14.5 % of all brain tumors and 48.6% of primary malignant brain tumors (2, 3). The expected median overall survival rate of persons with this kind of tumor is 6–14 months (4) and the annual incidences of GBM account for 3.19–4.17 cases/100,000 person/year (3, 5, 6). Some studies suggested that age and gender are important factors in glioma development (7, 8). The treatment approach varies depending on the type

of tumor and typically involves a mix of surgery, chemotherapy, and radiation (9, 10). Despite decades of research, GBM remains a formidable and deadly cancer. Current treatment approaches face limitations, such as drug resistance, molecular heterogeneity, and aberrant activation of different signaling pathways (1, 11). Severe adverse effects of the treatments currently in use for patients with GBM also pose a serious problem (12, 13). This prompts an urgent need for new therapies. Available pharmacological agents also face the problem of crossing the blood–brain barrier (14). Some promising drugs for first-line treatment are currently under development (15, 16). The correct strategy for brain tumor treatment should be to target the selective pathways that can give long-term therapeutic effects (10).

Nitric oxide (NO) is a small gaseous molecule that plays a significant role in various biological processes (17). It is crucial in regulating vascular function (such as vascular permeability, vasodilation, and angiogenesis), neural system development, neurotransmission, smooth muscle relaxation, immune responses, and cytotoxic functions (18). We have shown that excessive NO is implicated in the development of many neurodevelopmental, neurodegenerative, and neuropsychiatric disorders (19–27). NO is synthesized by inducible, endothelial, and neuronal nitric oxide synthase (iNOS, eNOS, and nNOS, respectively) (17). Increased activity of NOS enzymes and nitrosative stress are major culprits for developing many cancers (28, 29). Meanwhile, NOS inhibitors have been reported to alleviate different kinds of cancers, such as metastatic melanoma (30), human breast cancer (31), ovarian cancer (32), oral cell carcinoma (33), head and neck cancer (34), colon cancer (35, 36), and others. The cellular phenotypes and behaviors are impacted by the elevated NO present in the tumor microenvironment. In GBM, elevated NO levels are associated with advanced stages and reduced patient survival rate (37). NO involvement in cancer was reported long ago (38), but its exact mechanism is controversial and vague (37).

Excessive NO concentration leads to increased nitrosative and oxidative stress, which results in DNA strand breakage by alkylation and deamination of the nucleic acid bases in DNA (39). Aberrant NO also inhibits the activity of DNA repair enzymes (40). These changes enhance the neoplastic transformation and inhibition of apoptosis, promoting cancer development (41).

NO can induce both protumorigenic and antitumorigenic effects depending on its levels and physiological conditions (42). In GBM, NO generation by tumor cells may facilitate a progrowth environment for tumor cell proliferation and neovascularization (42). In gliomas, iNOS and nNOS have been found to promote glioma stem cell growth (43), develop temozolomide (TMZ) treatment resistance, and modulate the immune response. NO is also known to inhibit apoptosis via S-nitrosylation or cyclic GMP-dependent pathways (44). NO can also inhibit catalase and cytochrome P-450 and can cause redox imbalance and oxidative stress (44). Identifying the molecules targeting NO and NO-affected molecular pathways in GBM could be a novel target for the brain tumor study.

Our previous in vitro experiments targeting iNOS and nNOS with inhibitors have shown a marked reduction in U-87 MG cell proliferation (45). The current study (Figure 1) was designed to assess iNOS and nNOS inhibition as a therapeutic approach for GBM in vivo. We also compared the efficacy of this approach with the well-known antitumor drug TMZ and evaluated the effects of the combined action of BA-101 and TMZ.

Results

NOS Inhibition Reduces Tumor Growth in GBM Mice

The effects of pharmacological inhibition of nNOS and iNOS on tumor size and volume in mice were studied compared to vehicle-treated mice. In this set of experiments, we treated the mice with NOS inhibitors for 8 days. BA-103 reduced tumor size when compared to vehicle-treated mice. BA-101 also significantly reduced tumor growth compared to the vehicle group. Furthermore, BA-101 inhibited tumor growth at a



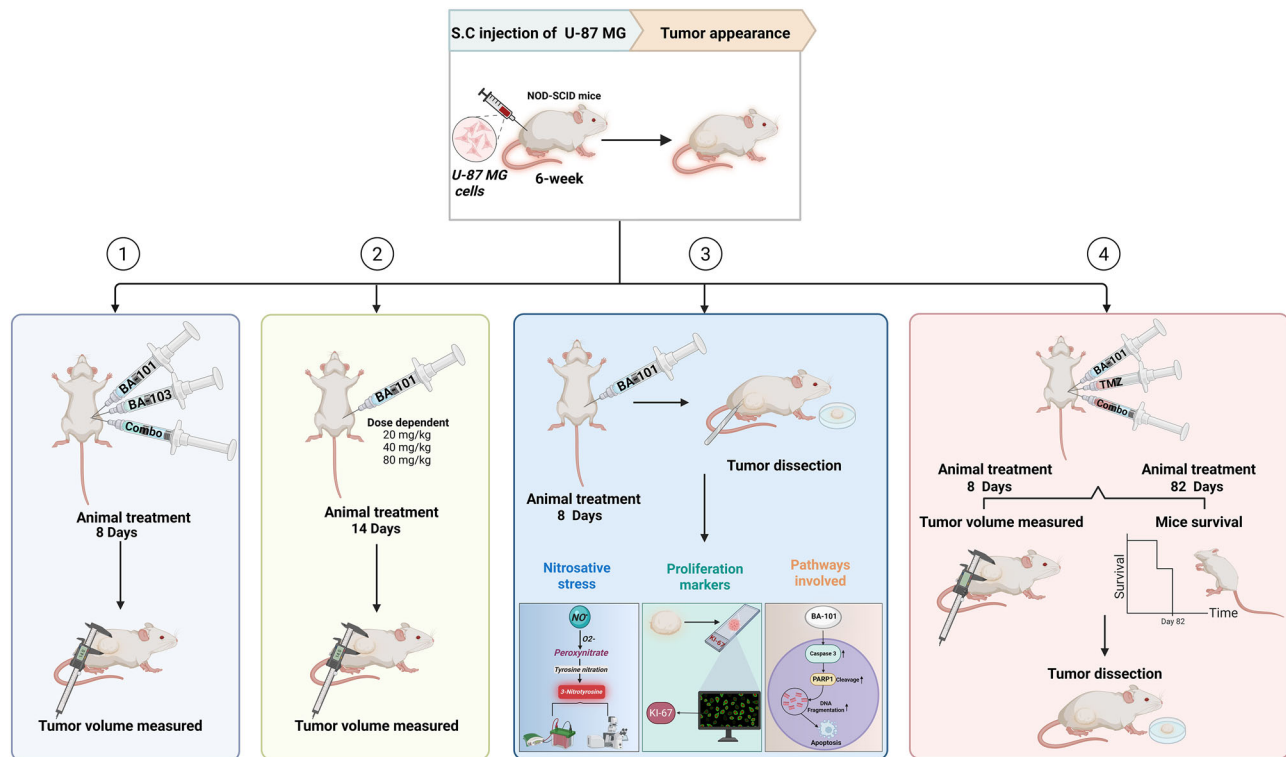


Figure 1. Schematic representation of the study. 6-week-old NOD-SCID male mice were injected with U-87 MG cells (1×10^6). Animals were treated with drugs or vehicles when tumors were developed. Tumor volumes were measured during different days of the experiment. The animals were sacrificed, and the tumors were isolated at the end of the experiment. WB and IF assays were performed to evaluate nitrosative stress and cell degradation processes.

considerably greater extent than BA-103. A combined treatment of BA-101 and BA-103 showed a marked reduction in tumor size compared to BA-101 or BA-103 treatment alone (Figure 2A and B). These results imply that both NOS inhibitors prevent tumor growth, but BA-101 was more effective than BA-103. Body weight analysis did not significantly change in all groups (Figure 2C). Tumor volume determination in real-time analysis showed that the tumors grew gradually in the vehicle group. Following the treatments with BA-103 and BA-101, the tumor growth was slower than in the vehicle group (Figure 2D).

The Dose-dependent Antitumor Effect of BA-101

We performed a dose-dependent study of BA-101, which appeared to be more effective in inhibiting the glioblastoma tumor volume than BA-103. Three doses of this compound were assessed, 20, 40, and 80 mg/kg. These treatments of BA-101 were given to mice daily for 14 days after the tumor size reached around 50 mm³. All three doses of BA-101 reduced the tumor volume (Figure 3B and D) and tumor weight (Figure 3C) compared to the vehicle group and this effect was dose dependent with the most potent reduction of tumor growth at 80 mg/kg. The serial determination of the tumor volume on different days of the experiment showed that the tumor size in the vehicle group grew faster than in the treatment groups, reaching a statistically significant difference already on the fifth day (Figure 3D).

Effects of BA-101 on Cell Proliferation, DNA Damage, Nitrosative Stress, and Apoptosis in GBM Mice

Treatment of mice with 80 mg/kg BA-101 showed a reduction in the tumor proliferating marker Ki-67 levels compared to the vehicle group (Figure 4A). The nitrosative stress marker 3-Ntyr was reduced 2-fold in the BA-101-treated mice compared to the vehicle-treated group (Figure 4B and C). The DNA degradation marker, cleaved PARP1, appeared to be doubled in mice subjected to the BA-101 treatment compared to the vehicle group (Figure 4D). The apoptotic marker, cleaved caspase 3, was also significantly increased by the BA-101 treatment (Figure 4E). These results

show that BA-101 treatment effectively reduced tumor proliferation and nitrosative stress while promoting DNA damage and apoptosis.

Effects of the Combined Treatment with BA-101 and TMZ on Tumor Growth

Then, the efficacy of BA-101 was compared to the TMZ, the gold standard of glioblastoma chemotherapy (46). We treated the mice with tumors daily for 8 days with BA-101 or TMZ or in combination with both (TMZ and BA-101). BA-101 and TMZ alone significantly reduced tumor size at a similar extent. However, treatment of GBM mice with the combination of TMZ and BA-101 provided a dramatically more significant reduction in the tumor volume than in the vehicle-treated groups (Figure 5A and B). Thus, tumor volume in the BA-101 + TMZ group of mice was reduced 6-fold, while in the BA-101 and TMZ groups, the reduction reached 50% and 60%, respectively. Real-time tumor volume analysis revealed consistent growth in the vehicle-treated group, whereas treatment with BA-101, TMZ, or their combination significantly reduced tumor growth. The most pronounced effect was observed in mice receiving the combination therapy (Figure 5C). We also tested the survival of mice after treatment with BA-101, TMZ, and the combination of BA-101 and TMZ. In the survival study, we treated the tumor-bearing mice with BA-101 daily and TMZ for 5 days a week in a 2-weeks-on, 2-weeks-off cycle until the mice reached the end of their survival period. The expected number of survival days (probability of survival) was the highest in the combo treatment with BA-101 and TMZ compared to the treatment of GBM mice with both the vehicle and either of these drugs alone (Figure 5D).

Materials and Methods

Materials

Primary antibodies anti-Ki-67 (AB16667) from Abcam, anti-cleaved caspase 3 (#9661) and secondary antibodies, anti-rabbit Alexa fluor 594 (#8889), anti-mouse Alexa Fluor 488 (#4408), Horseradish peroxidase (HRP)-conjugated anti-rabbit (70765), HRP-conjugated anti-mouse (70745), ProLong Gold Antifade with the nucleus marker DAPI

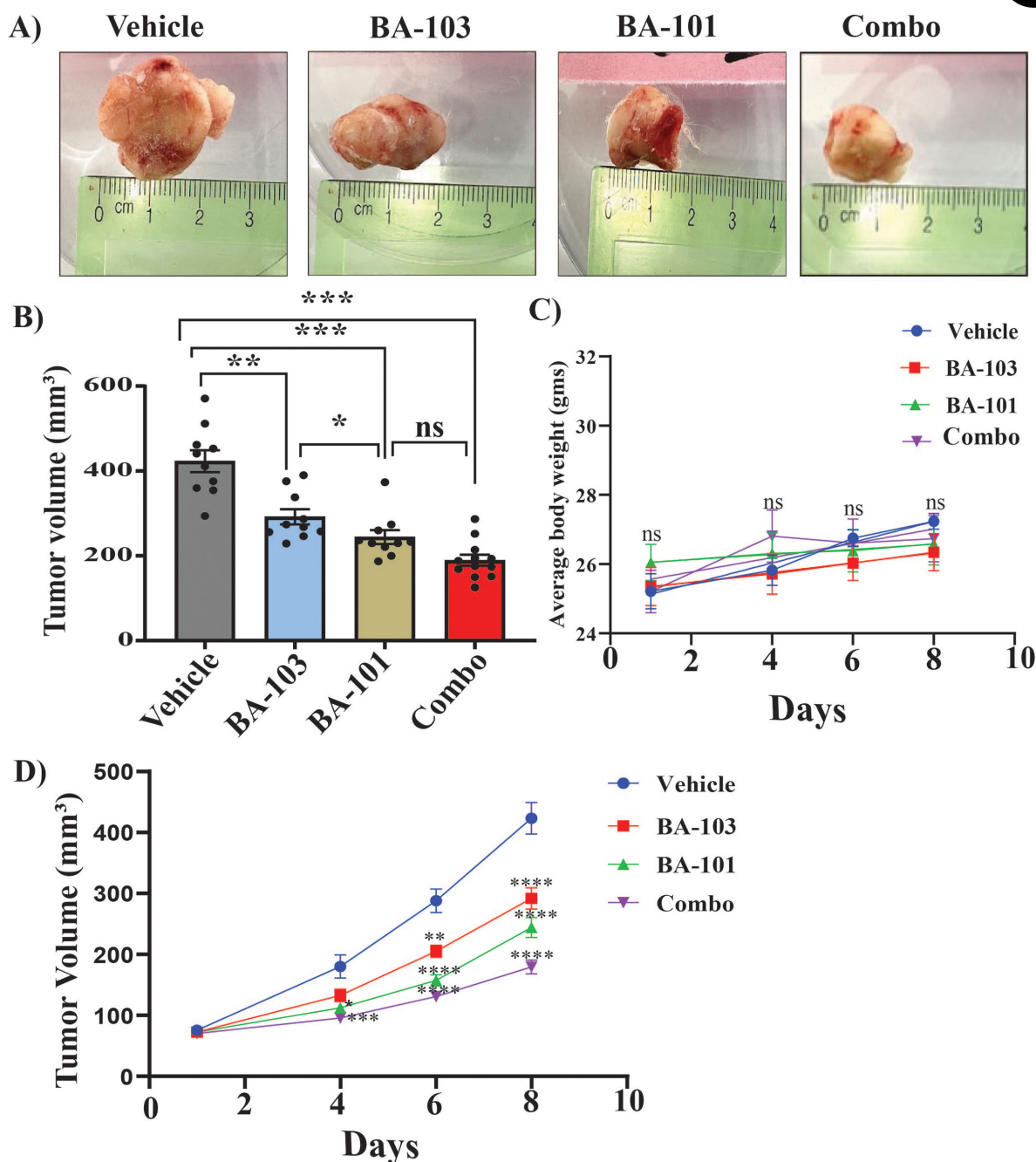


Figure 2. NOS inhibition prevents tumor growth in glioblastoma. (A) Representative tumor images in the Vehicle ($n = 10$), BA-103 ($n = 10$), BA-101 ($n = 10$), and BA-101 + BA-103 (Combo) ($n = 12$) groups of mice. (B) Statistical analysis of tumor volume in the groups mentioned above. (C) Statistical analysis of the dynamics of body weight changes in the above groups of mice during the experiment. (D) Statistical analysis of the dynamics of tumor volume changes in mice treated with vehicle ($n = 10$), BA-103 ($n = 10$), BA-101 ($n = 10$), and BA-103 + BA-101 ($n = 12$) during the experiment. Data are presented as mean \pm SEM. **** $P < 0.0001$, *** $P < 0.001$, ** $P < 0.01$, * $P < 0.05$, and ns, not significant.

(#8961), and protease phosphatase inhibitor cocktail (#5872) were purchased from Cell Signaling Technology (Danvers, MA, USA). Primary antibody anti-3-nitrotyrosine (3-Ntyr) (AB110282) was procured from Abcam (Cambridge, UK). Primary antibodies, anti-PARP1 (SC-56196) were purchased from Santa Cruz Biotechnology Inc. Other general chemicals were purchased from Sigma-Aldrich (St. Louis, MO, USA) and Bio-Rad Laboratories (Hercules, CA, USA).

The chemical identities of compounds BA-101 and BA-103 will be made available upon patent issuance. Patent applications covering the novel therapeutic use of these previously known molecules have been

filed. Researchers interested in obtaining the compounds for research purposes after patent issuance should contact the corresponding author. We truly believe in data reproducibility and eager to uncover the names of the molecules as stated above.

Animals

All animal experiments were conducted under the guidelines of the Institutional Animal Care Committee of the Hebrew University of Jerusalem and Use Committee and the Association for Assessment and Accreditation of Laboratory Animal Care International. The ethical approval (IACUC-

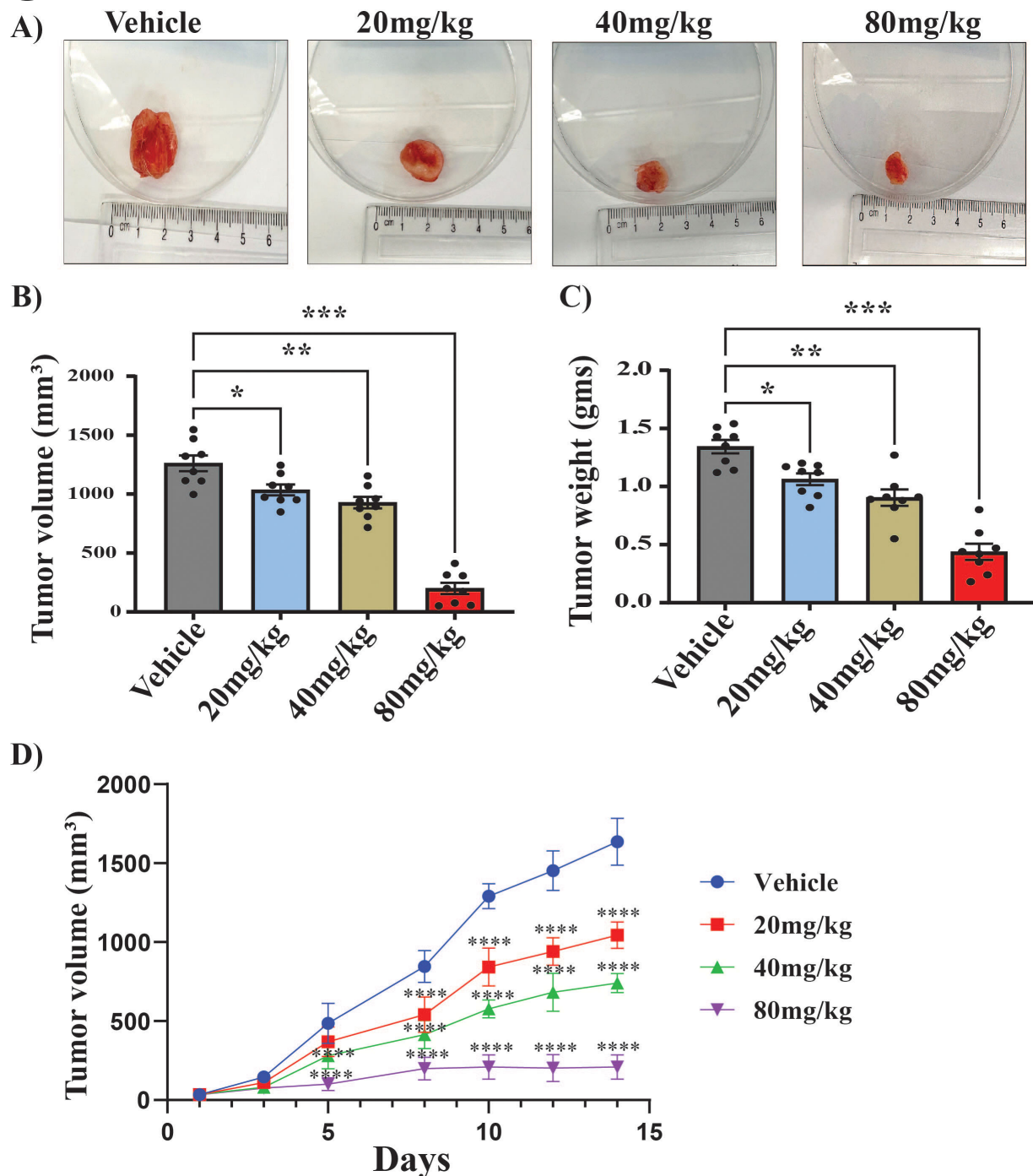


Figure 3. Dose-dependent treatment with BA-101. (A) Representative tumor images after dissection of the tumors in the dose-response study of BA-101. (B) Statistical analysis of tumor volume in mice treated with vehicle, and 20, 40, and 80 mg/kg of BA-101. (C) Statistical analysis of tumor weight in mice treated with vehicle (n = 8), and 20 mg/kg (n = 8), 40 mg/kg (n = 8), and 80 mg/kg of BA-101 (n = 8) on different days during the treatment. Data are presented as mean \pm SEM. *****P* < 0.0001, ****P* < 0.001, ***P* < 0.01, and **P* < 0.05.

MD-23-17231-5) was granted by the Hebrew University of Jerusalem. This study is reported under ARRIVE guidelines. Five-week-old NOD.CB17-Prkdc-scld/NCrHsd male mice were purchased from Envigo.

Glioblastoma Cell Line

Uppsala 87 Malignant Glioma (U-87 MG) cell line was obtained from the American Type Culture Collection (ATCC) and maintained in Dulbecco's modified Eagle medium (DMEM, Gibco 41965-039), 10% fe-

tal bovine serum (FBS, Gibco 10270-106), 1% penicillin/streptomycin, 10,000 U/mL (Pen/Strep, Gibco 15140-122) in the humidified atmosphere (37°C, 5% CO₂).

Generation of Subcutaneous Glioblastoma Xenograft Model and Drug Treatment

Subcutaneous glioblastoma-bearing mice were obtained by subcutaneous injection of 1×10^6 U-87 MG cells in 100 μ L PBS into the flanks of

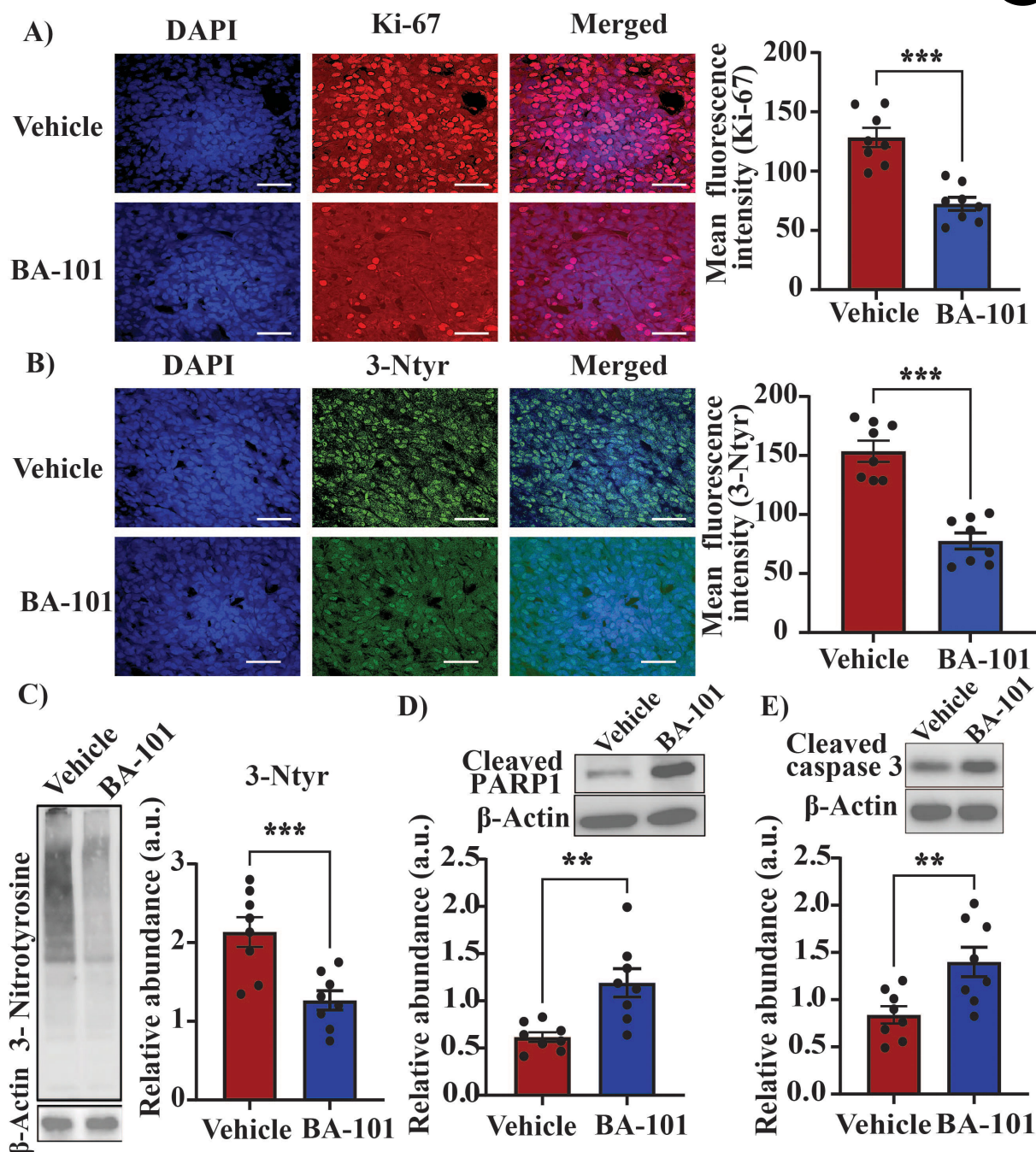


Figure 4. NOS inhibition with BA-101 induces apoptosis and reduces nitrosative stress. (A) Left: Representative confocal images of Ki-67 and DAPI in tumor sections of mice with Vehicle and BA-101(80 mg/kg) groups. The images were captured at 40 × magnification. Right: Statistical analysis of the mean fluorescence intensity of Ki-67 in both groups. (B) Left: Representative confocal images of 3-Ntyr and DAPI in tumor sections of mice of Vehicle and BA-101 groups. The image was captured at 40 × magnification. The scale bar in all images = 50 μm. Right: Statistical analysis of the mean fluorescence intensity of 3-Ntyr in both groups. (C) A representative WB image of 3-Ntyr and its quantitative analysis in Vehicle and BA-101 groups of mice. (D) A representative WB of DNA degradation marker PARP1 and its quantitative analysis in Vehicle and BA-101 groups. (E) Representative WB of cleaved caspase 3 protein and its quantitative analysis in Vehicle and BA-101 groups of mice. Data are presented as mean ± SEM. $n = 8$ in each group. *** $P < 0.001$, and ** $P < 0.01$.

6-week-old male NOD.CB17-Prkdc-scld/NCrHsd (NOD-SCID) mice. Then, 2–3 weeks after tumor cell implantation, when the average tumor size reached approximately 50 mm³, mice were randomly divided into four groups, with 6–10 mice per group. Animals were treated intraperitoneally with a vehicle, BA-103 (10 mg/kg), BA-101 (80 mg/kg), or TMZ (10 mg/kg) in 100 μl of PBS containing 5% DMSO. All mice were sacrificed after the tumor size reached 1.5 cm in either of the dimensions. Tumor tissues were

surgically excised, either stored at –80°C or fixed with 4% paraformaldehyde solution, dehydrated, and used for cryosectioning.

Tumor Growth and Probability of Survival

The tumor growth was assessed by measuring the tumor weight and volume. The mouse body weight and tumor size were measured every other day during the experiments. The tumor volume was measured with a digital caliper and calculated with the following formula: tumor

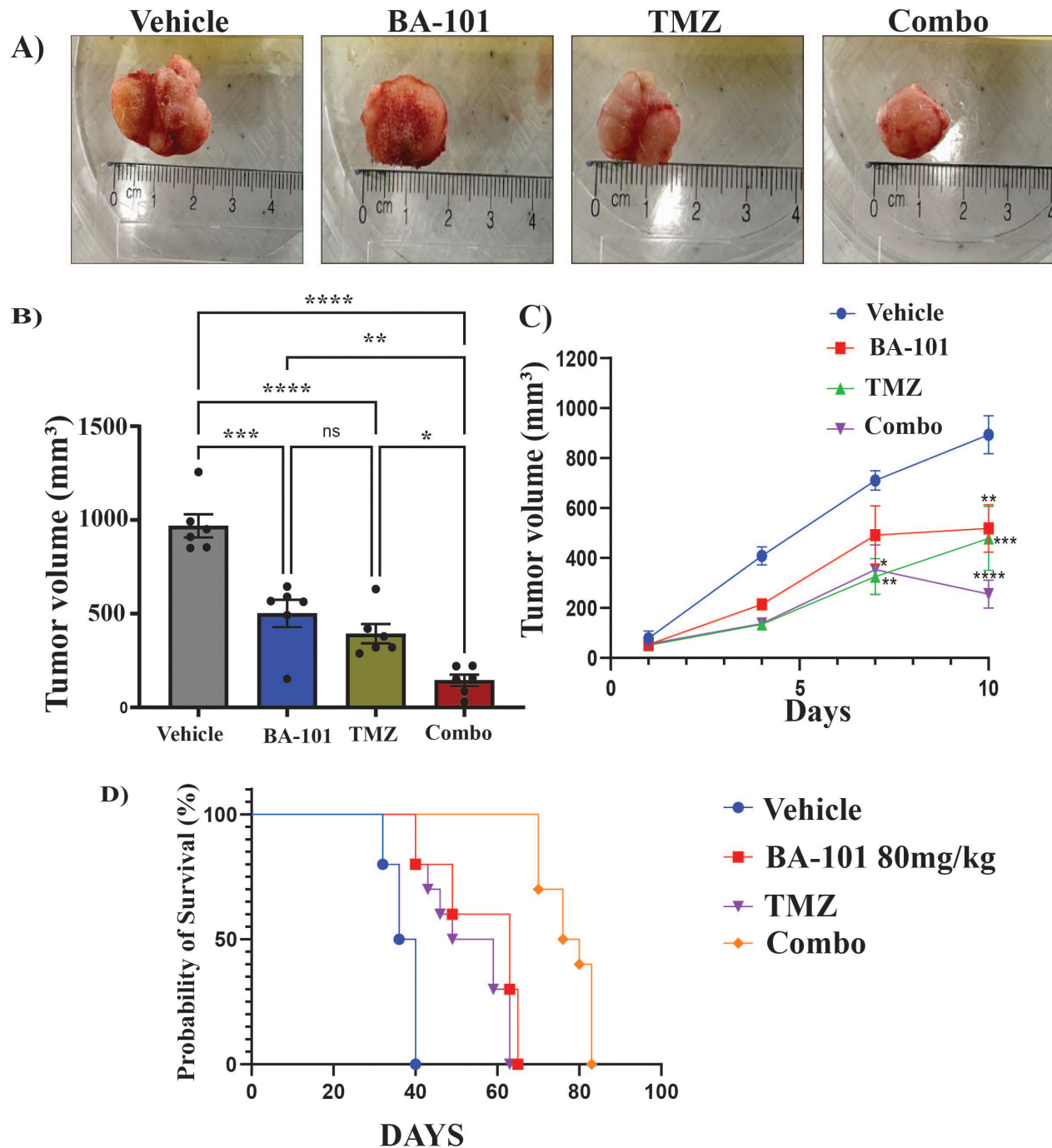


Figure 5. Combo treatment of TMZ and BA-101 increases survivability. (A) Representative tumor images after dissection in Vehicle, BA-101 (80 mg/kg), TMZ, and BA-101 + TMZ (Combo) groups. (B) Statistical analysis of tumor volume in Vehicle, BA-101, TMZ, and BA-101 + TMZ groups. (C) Statistical analysis of tumor volume growth comparison in Vehicle (*n* = 6), BA-101 (*n* = 6), TMZ (*n* = 6), and BA-101 + TMZ (*n* = 6) groups on different days during the treatment. (D) Kaplan-Meier plot for mice harboring U-87 MG glioblastoma xenografts treated with Vehicle (*n* = 6), BA-101 (*n* = 6), TMZ (*n* = 6), and BA-101 + TMZ (*n* = 6). Data are presented as mean \pm SEM. *****P* < 0.0001, ****P* < 0.001, ***P* < 0.01, **P* < 0.05, and ns, not significant.

volume = (length \times width²)/2. The probability of survival was determined when the tumor size was 1.5 cm in either dimension, length, or width.

Western Blots

The tissues were homogenized in a freshly prepared RIPA buffer as described previously (22). It contained 30 mM HEPES (pH 7.4), 150 mM NaCl, 1% Nonidet P-40, 0.5% sodium deoxycholate, 0.1% sodium dodecyl sulfate, 5 mM EDTA, 1 mM Na₃VO₄, 50 mM NaF, 1 mM PMSF, and 1%

protease/phosphatase inhibitors cocktail (pH 7.7). All these chemicals were purchased from Sigma-Aldrich. Homogenization was performed on ice using a Teflon pestle and a Jumbo stirrer from Thermo Fisher Scientific (Waltham, MA, USA). The homogenates underwent centrifugation at 17,000 \times *g* for 30 min at a temperature of 4°C. The supernatant of the sample was collected, and the protein concentration was determined using the bicinchoninic acid protein assay kit provided by Sigma-Aldrich. The samples underwent polyacrylamide gel electrophoresis, after which they were transferred onto a Polyvinylidene difluoride (PVDF) membrane using



a semidry transfer method (Bio-Rad Laboratories). Nonspecific sites were effectively blocked by 5% dried skimmed milk in Tris-buffered saline with Tween 20 (TBST). The TBST solution consisted of 135 mM NaCl, 50 mM Tris, and 0.1% Tween 20, pH 7.4. This blocking process was carried out for 2 h at room temperature. PVDF membranes containing the transferred proteins were incubated overnight at 4°C on a shaker with a primary antibody. Primary antibodies used were anti-3-Ntyr [diluted 1:1000 for Western blots (WB) and 1:200 for immunofluorescence (IF)], anti-cleaved caspase 3 (diluted 1:1000), anti-cleaved PARP1 (diluted 1:1000), and anti- β -actin (diluted 1:1000). Following the exposure to primary antibodies, the membranes underwent a washing step with TBST for three times 10 min each followed by an incubation process with anti-mouse/rabbit HRP-conjugated secondary antibody for 1 h at ambient temperature. The specific binding of the protein was identified using an ECL substrate manufactured by Bio-Rad Laboratories. The bands were acquired using the Bio-Rad Chemidoc imaging system as described previously (22).

IF and Confocal Microscopy

After dissection, the tumors were directly preserved in a 4% paraformaldehyde solution for 2 days. After fixation, the tumors were gradually dehydrated with 10%, 20%, 30%, sucrose solution. Using cryostats, the 20- μ m-thick tumor section was cut. The tumor sections were processed for IF. The sections were incubated in a blocking buffer followed by anti-rabbit Ki-67 (diluted 1:500), and 3-Ntyr (diluted 1:200) primary antibodies. Then, the sections were rinsed with PBS and incubated with anti-rabbit Alexa Fluor 594 (diluted 1:1000) and anti-mouse Alexa Fluor 488 (diluted 1:1000) secondary antibodies for 2 h in the dark. After the incubation with secondary antibodies, sections were washed with PBS three times and mounted on glass slides with DAPI. Images were captured at 40X using a Nikon confocal microscope.

Statistical Analysis

Statistical analysis was performed using GraphPad Prism Software, v. 9.3 (San Diego, CA, USA). Data are presented as mean \pm SEM. A two-way ANOVA followed by Tukey's multiple comparison tests was performed to analyze body weight and tumor volume on different days during the experiment. A one-way ANOVA followed by Tukey's multiple comparison test was used for the group comparisons to measure tumor volume at the end of the experiment. An unpaired *t* test was used for WB and IF. The differences between the groups were considered statistically significant at *P* < 0.05.

Discussion

Our recent study on GBM proved the involvement of nitric oxide in tumor progression and showed that NOS inhibition can prevent tumor proliferation in vitro. A study by Kruglyakov *et al.* showed that NOS inhibitors reduced GBM cell proliferation in vitro (45). The current study investigates the efficacy of NOS inhibitors in the xenograft mouse model of GBM.

Overexpression of nNOS has been reported in GBM patient samples (47). Another study also found higher nNOS activity in high-grade glioma (48). This shows the significant link between malignancy in glial tumors and NO overproduction, which can be associated with the overexpression of nNOS or its elevated activity. iNOS inhibitors have also been found to be effective in some studies for GBM treatment (49, 50).

Treatment of the xenograft mouse model of GBM with BA-103 and BA-101 in our experiments reduced tumor weight and volume, showing that NOS is implicated in cell death and tumor growth in this kind of cancer. Real-time tumor progression data showed that tumor growth was significantly inhibited by BA-103, BA-101, or the mixture of these two drugs. BA-101 appeared to be more effective in tumor volume reduction than BA-103. Combined treatment with BA-103 and BA-101 provided a more potent preventive effect on tumor growth. Further body weight measurement in all groups showed no difference. Since BA-101 displayed higher efficacy in inhibiting tumor growth than BA-103, we chose this NOS inhibitor for a dose-response study to find the most effective dose of BA-101 for treatment. BA-101 inhibited tumor growth at all doses used in this study, from 20 to 80 mg/kg. This effect was dose dependent, with the most significant inhibition of tumor progression among the doses tested being achieved at 80 mg/kg.

A nuclear protein, Ki-67, is widely used as a proliferation marker (51). Its expression correlates directly with metastasis and clinical tumor stage (52). We found that the treatment of mice with BA-101 at a dose of 80 mg/kg had lower expression of Ki-67 than the vehicle-treated group, indicating the lower proliferation of the tumor cells. Apoptosis ensures the homeostatic balance between cell proliferation and death (53–55). It represents a molecular pathway of self-destruction to eliminate the damaged or failing cells and subcellular structures and molecules and to allow their repair or replacement (56). BA-101 treatment considerably increased the cleaved caspase 3 and cleaved PARP1 levels, indicating augmented apoptosis and DNA degradation. Activation of these self-destruction processes was likely associated with the tumor volume and size growth suppression in the GBM model used in this study. Notably, the link between DNA degradation and apoptosis has been previously found, and these processes might be followed by cell detoxification and repair (57). Inhibiting nNOS can trigger apoptosis in glioblastoma cells. Reducing NO levels through nNOS inhibition disrupts survival pathways, leading to programmed cell death. This mechanism is crucial, as glioblastomas often evade apoptosis, contributing to their malignancy (58).

Further, we assessed the nitrosative stress marker 3-Ntyr levels in tumor sections. 3-Ntyr is formed by the nitration of tyrosine residues in both protein-bound and free forms by reactive peroxynitrite molecules (59). In this study, both WB and IF confirmed a reduction in 3-Ntyr levels and consequently reduced nitrosative stress in the BA-101 treatment group.

TMZ is a monofunctional DNA alkylating agent employed to treat patients with newly diagnosed GBM (60). It is a lipophilic molecule with oral administration feasibility, which can effectively cross the blood-brain barrier (61). TMZ has been a gold standard drug for GBM treatment (46). We compared the ability of BA-101 and TMZ alone and in combination to inhibit tumor growth. The reduction in tumor volume was greater in GBM mice treated with the combination of the two drugs compared to BA-101 or TMZ alone. nNOS inhibition has been shown to sensitize glioblastoma cells to chemotherapeutic agents like TMZ. Pretreatment with nNOS inhibitors decreased cell viability in glioblastoma cells exposed to TMZ (58).

The limitations of this study were that it did not include the pharmacodynamic assessments required for early-phase clinical trials to evaluate the safety and efficacy of BA-101 in patients with GBM. We consider the hurdles in clinical translation, such as variability in patient response, potential toxicity, and the need for optimized dosing regimens. This study serves as a proof of concept demonstrating the involvement of nitric oxide synthase (NOS) in GBM pathophysiology. It provides a strong foundation for future investigations to refine therapeutic strategies and advance clinical translation.

In conclusion, this study showed that NO synthesis overactivation in GBM, particularly neuronal NO production, could be an essential pathogenic factor of tumor growth. The selective nNOS inhibitor BA-101 or its combination with TMZ might be a prospective therapeutic agent for GBM treatment. Further studies are required to assess the safety and efficacy of this novel therapeutic approach in patients with GBM.

Data Availability Statement

The data that support the findings of this study are available on request from the corresponding author. The data are not publicly available due to privacy or ethical restrictions.

Acknowledgments

We thank the Satell Family Foundation and the Neubauer Family Foundation for their support.

Authors Contributions

S.K.O.: Animals' handling, biochemical analysis, and writing paper. M.K.T.: Animals' handling. W.B.: Animals' handling and biochemical analysis. M.K.: Contributing to the Discussion. S.G.: Data analysis. A.M.: Data analysis. M.N.: Animals' handling. I.K.: Contributing to the Discussion. H.A.: Study planning, idea conceptualization, and research supervision.

Funding Sources

This work was funded partly by NeuroNOS Ltd. and the Berettler Centre for Research in Molecular Pharmacology and Therapeutics Grant.



Author Disclosures

H.A. is a CSO of Point6 Bio and Neuro-NOS Ltd. Funds were received from Neuro-NOS Ltd. No funds from Point6 Bio were received for this study. NeuroNOS Ltd. has obtained a license for patent applications of both molecules filed by Yissum (The Hebrew University Tech Transfer Company). All other authors do not hold any competing interests.

References

- Wu W, Klockow JL, Zhang M, Lafortune F, Chang E, Jin L, et al. Glioblastoma multiforme (GBM): an overview of current therapies and mechanisms of resistance. *Pharmacol Res.* 2021;171:105780. DOI: [10.1016/j.phrs.2021.105780](https://doi.org/10.1016/j.phrs.2021.105780). PMID: 34302977; PMCID: [PMC8384724](https://pubmed.ncbi.nlm.nih.gov/PMC8384724/)
- Hanif F, Muzaffar K, Perveen K, Malhi SM, Simjee ShU. Glioblastoma multiforme: a review of its epidemiology and pathogenesis through clinical presentation and treatment. *Asian Pac J Cancer Prev.* 2017;18(1):3–9. DOI: [10.22034/APJCP.2017.18.1.3](https://doi.org/10.22034/APJCP.2017.18.1.3). PMID: 28239999; PMCID: [PMC5563115](https://pubmed.ncbi.nlm.nih.gov/PMC5563115/)
- Grochans S, Cybulska AM, Simińska D, Korbecki J, Kojder K, Chlubek D, et al. Epidemiology of glioblastoma multiforme—literature review. *Cancers.* 2022;14:2412. DOI: [10.3390/cancers14102412](https://doi.org/10.3390/cancers14102412). PMID: 35626018; PMCID: [PMC9139611](https://pubmed.ncbi.nlm.nih.gov/PMC9139611/)
- Mohammed S, Dinesan M, Ajayakumar T. Survival and quality of life analysis in glioblastoma multiforme with adjuvant chemoradiotherapy: a retrospective study. *Rep Pract Oncol Radiother.* 2022;27(6):1026–36. DOI: [10.5603/RPOR.a2022.0113](https://doi.org/10.5603/RPOR.a2022.0113). PMID: 36632307; PMCID: [PMC9826661](https://pubmed.ncbi.nlm.nih.gov/PMC9826661/)
- Batash R, Asna N, Schaffer P, Francis N, Schaffer M. Glioblastoma multiforme, diagnosis and treatment; recent literature review. *Curr Med Chem.* 2017;24(27):3002–9. DOI: [10.2174/0929867324666170516123206](https://doi.org/10.2174/0929867324666170516123206). PMID: 28521700
- Fabbro-Peray P, Zouaoui S, Darlix A, Fabbro M, Pallud J, Rigau V, et al. Association of patterns of care, prognostic factors, and use of radiotherapy-temozolomide therapy with survival in patients with newly diagnosed glioblastoma: a French national population-based study. *J Neurooncol.* 2019;142(1):91–101. DOI: [10.1007/s11060-018-03065-z](https://doi.org/10.1007/s11060-018-03065-z). PMID: 30523606; PMCID: [PMC6399437](https://pubmed.ncbi.nlm.nih.gov/PMC6399437/)
- Tian M, Ma W, Chen Y, Yu Y, Zhu D, Shi J, et al. Impact of gender on the survival of patients with glioblastoma. *Biosci Rep.* 2018;38(6):BSR20180752. DOI: [10.1042/BSR20180752](https://doi.org/10.1042/BSR20180752). PMID: 30305382; PMCID: [PMC6239255](https://pubmed.ncbi.nlm.nih.gov/PMC6239255/)
- Li K, Lu D, Guo Y, Wang C, Liu X, Liu Yu, et al. Trends and patterns of incidence of diffuse glioma in adults in the United States, 1973–2014. *Cancer Med.* 2018;7(10):S281–90. DOI: [10.1002/cam4.1757](https://doi.org/10.1002/cam4.1757). PMID: 30175510; PMCID: [PMC6198197](https://pubmed.ncbi.nlm.nih.gov/PMC6198197/)
- Schaff LR, Mellinghoff IK. Glioblastoma and other primary brain malignancies in adults: a review. *JAMA.* 2023;329(7):574–87. DOI: [10.1001/jama.2023.0023](https://doi.org/10.1001/jama.2023.0023). PMID: 36809318; PMCID: [PMC11445779](https://pubmed.ncbi.nlm.nih.gov/PMC11445779/)
- Angom RS, Nakka NM, Bhattacharya S. Advances in glioblastoma therapy: an update on current approaches. *Brain Sci.* 2023;13:1536. DOI: [10.3390/brainsci13111536](https://doi.org/10.3390/brainsci13111536). PMID: 38002496; PMCID: [PMC10669378](https://pubmed.ncbi.nlm.nih.gov/PMC10669378/)
- Qazi MA, Vora P, Venugopal C, Sidhu SS, Moffat J, Swanton C, et al. Intratumoral heterogeneity: pathways to treatment resistance and relapse in human glioblastoma. *Ann Oncol.* 2017;28(7):1448–56. DOI: [10.1093/annonc/mdx169](https://doi.org/10.1093/annonc/mdx169). PMID: 28407030
- Omuro A, DeAngelis LM. Glioblastoma and other malignant gliomas: a clinical review. *JAMA.* 2013;310(17):1842–50. DOI: [10.1001/jama.2013.280319](https://doi.org/10.1001/jama.2013.280319). PMID: 24193082
- McKinnon C, Nandhabalan M, Murray SA, Plaha P. Glioblastoma: clinical presentation, diagnosis, and management. *BMJ.* 2021;374:n1560. DOI: [10.1136/bmj.n1560](https://doi.org/10.1136/bmj.n1560). PMID: 34261630
- Kim S-S, Harford JB, Pirolo KF, Chang EH. Effective treatment of glioblastoma requires crossing the blood-brain barrier and targeting tumors including cancer stem cells: the promise of nanomedicine. *Biochem Biophys Res Commun.* 2015;468(3):485–9. DOI: [10.1016/j.bbrc.2015.06.137](https://doi.org/10.1016/j.bbrc.2015.06.137). PMID: 26116770; PMCID: [PMC4690805](https://pubmed.ncbi.nlm.nih.gov/PMC4690805/)
- Shergalis A, Bankhead A, Luesakul U, Muangsing N, Neamat N. Current challenges and opportunities in treating glioblastoma. *Pharmacol Rev.* 2018;70(3):412–45. DOI: [10.1124/pr.117.014944](https://doi.org/10.1124/pr.117.014944). PMID: 29669750; PMCID: [PMC5907910](https://pubmed.ncbi.nlm.nih.gov/PMC5907910/)
- Oronsky B, Reid TR, Oronsky A, Sandhu N, Knox SJ. A review of newly diagnosed glioblastoma. *Front Oncol.* 2020;10:574012. DOI: [10.3389/fonc.2020.574012](https://doi.org/10.3389/fonc.2020.574012). PMID: 33614476; PMCID: [PMC7892469](https://pubmed.ncbi.nlm.nih.gov/PMC7892469/)
- Tripathi MK, Kartawy M, Amal H. The role of nitric oxide in brain disorders: autism spectrum disorder and other psychiatric, neurological, and neurodegenerative disorders. *Redox Biol.* 2020;34:101567. DOI: [10.1016/j.redox.2020.101567](https://doi.org/10.1016/j.redox.2020.101567). PMID: 32464501; PMCID: [PMC7256645](https://pubmed.ncbi.nlm.nih.gov/PMC7256645/)
- Reddy TP, Glynn SA, Billiar TR, Wink DA, Chang JC. Targeting nitric oxide: say NO to metastasis. *Clin Cancer Res.* 2023;29(10):1855–68. DOI: [10.1158/1078-0432.CCR-22-2791](https://doi.org/10.1158/1078-0432.CCR-22-2791). PMID: 36520504; PMCID: [PMC10183809](https://pubmed.ncbi.nlm.nih.gov/PMC10183809/)
- Mencer S, Kartawy M, Lendenfeld F, Soluh H, Tripathi MK, Khaliulin I, et al. Proteomics of autism and Alzheimer's mouse models reveal common alterations in mTOR signaling pathway. *Transl Psychiatry.* 2021;11(1):480. DOI: [10.1038/s41398-021-01578-2](https://doi.org/10.1038/s41398-021-01578-2). PMID: 34535637; PMCID: [PMC8448888](https://pubmed.ncbi.nlm.nih.gov/PMC8448888/)
- Steinert JR, Amal H. The contribution of an imbalanced redox signalling to neurological and neurodegenerative conditions. *Free Radic Biol Med.* 2023;194:71–83. DOI: [10.1016/j.freeradbiomed.2022.11.035](https://doi.org/10.1016/j.freeradbiomed.2022.11.035). PMID: 36435368
- Tripathi MK, Kartawy M, Ginzburg S, Amal H. Arsenic alters nitric oxide signaling similar to autism spectrum disorder and Alzheimer's disease-associated mutations. *Transl Psychiatry.* 2022;12(1):127. DOI: [10.1038/s41398-022-01890-5](https://doi.org/10.1038/s41398-022-01890-5). PMID: 35351881; PMCID: [PMC8964747](https://pubmed.ncbi.nlm.nih.gov/PMC8964747/)
- Tripathi MK, Ojha SK, Kartawy M, Hamoudi W, Choudhary A, Stern S, et al. The NO answer for autism spectrum disorder. *Adv Sci.* 2023;10(22):2205783. DOI: [10.1002/adv.202205783](https://doi.org/10.1002/adv.202205783). PMID: 37212048; PMCID: [PMC10401098](https://pubmed.ncbi.nlm.nih.gov/PMC10401098/)
- Yang H, Oh C-Ki, Amal H, Wishnok JS, Lewis S, Schahrer E, et al. Mechanistic insight into female predominance in Alzheimer's disease based on aberrant protein S-nitrosylation of C3. *Sci Adv.* 2022;8(50):eade0764. DOI: [10.1126/sciadv.ade0764](https://doi.org/10.1126/sciadv.ade0764). PMID: 36516243; PMCID: [PMC9750152](https://pubmed.ncbi.nlm.nih.gov/PMC9750152/)
- Hamoudi W, Tripathi MK, Ojha SK, Amal H. A cross-talk between nitric oxide and the glutamatergic system in a Shank3 mouse model of autism. *Free Radical Biol Med.* 2022;188:83–91. DOI: [10.1016/j.freeradbiomed.2022.06.007](https://doi.org/10.1016/j.freeradbiomed.2022.06.007). PMID: 35716826
- Abdel-Haq M, Ojha SK, Hamoudi W, Kumar A, Tripathi MK, Khaliulin I, et al. Effects of extended-release 7-nitroindazole gel formulation treatment on the behavior of Shank3 mouse model of autism. *Nitric Oxide.* 2023;140:1–41–49. DOI: [10.1016/j.niox.2023.09.003](https://doi.org/10.1016/j.niox.2023.09.003). PMID: 37714296
- Bazbaz W, Kartawy M, Hamoudi W, Ojha SK, Khaliulin I, Amal H. The role of thioredoxin system in Shank3 mouse model of autism. *J Mol Neurosci.* 2024;74(4):90. DOI: [10.1007/s12031-024-02270-y](https://doi.org/10.1007/s12031-024-02270-y). PMID: 39347996; PMCID: [PMC11457715](https://pubmed.ncbi.nlm.nih.gov/PMC11457715/)
- Ojha SK, Amal H. Air pollution: an emerging risk factor for autism spectrum disorder. *Brain Med.* 2024;1–4.
- Ortega AL, Mena S, Estrela JM. Oxidative and nitrosative stress in the metastatic microenvironment. *Cancers.* 2010;2(2):274–30. DOI: [10.3390/cancers2020274](https://doi.org/10.3390/cancers2020274). PMID: 24281071; PMCID: [PMC3835079](https://pubmed.ncbi.nlm.nih.gov/PMC3835079/)
- Luanpitpong S, Chanvorachote P. Nitric oxide and aggressive behavior of lung cancer cells. *Anticancer Res.* 2015;35(9):4585–92. PMID: 26254346
- Ekmekcioglu S, Ellerhorst J, Smid CM, Prieto VG, Munsell M, Buzaid AC, et al. Inducible nitric oxide synthase and nitrotyrosine in human metastatic melanoma tumors correlate with poor survival. *Clin Cancer Res.* 2000;6(12):4768–75. PMID: 11156233
- Loibl S, Buck A, Strank C, von Minckwitz G, Roller M, Sinn H-P, et al. The role of early expression of inducible nitric oxide synthase in human breast cancer. *Eur J Cancer.* 2005;41(2):265–71. DOI: [10.1016/j.ejca.2004.07.010](https://doi.org/10.1016/j.ejca.2004.07.010). PMID: 15661552
- Raspollini MR, Amunni G, Villanuoci A, Boddi V, Baroni G, Taddei A, et al. Expression of inducible nitric oxide synthase and cyclooxygenase-2 in ovarian cancer: correlation with clinical outcome. *Gynecol Oncol.* 2004;92(3):806–12. DOI: [10.1016/j.ygyno.2003.12.023](https://doi.org/10.1016/j.ygyno.2003.12.023). PMID: 14984945
- Connelly ST, Macabeo-Ong M, Dekker N, Jordan RCK, Schmidt BL. Increased nitric oxide levels and iNOS over-expression in oral squamous cell carcinoma. *Oral Oncol.* 2005;41(3):261–7. DOI: [10.1016/j.oraloncology.2004.09.007](https://doi.org/10.1016/j.oraloncology.2004.09.007). PMID: 15743688
- Brennan PA, Dennis S, Poller D, Quintero M, Puxeddu R, Thomas GJ, et al. Inducible nitric oxide synthase: correlation with extracapsular spread and enhancement of tumor cell invasion in head and neck squamous cell carcinoma. *Head Neck.* 2008;30(2):208–14. DOI: [10.1002/hed.20675](https://doi.org/10.1002/hed.20675). PMID: 17657783
- Ahn B, Ohshima H. Suppression of intestinal polyposis in Apc(Min/+) mice by inhibiting nitric oxide production. *Cancer Res.* 2001;61(23):8357–60. PMID: 11731407
- Kawamori T, Takahashi M, Watanabe K, Ohta T, Nakatsugi S, Sugimura T, et al. Suppression of azoxymethane-induced colonic aberrant crypt foci by a nitric oxide synthase inhibitor. *Cancer Lett.* 2000;148(1):33–7. DOI: [10.1016/S0304-3835\(99\)00310-9](https://doi.org/10.1016/S0304-3835(99)00310-9). PMID: 10680590
- Tran AN, Boyd NH, Walker K, Hjelmeland AB. NOS expression and NO function in glioma and implications for patient therapies. *Antioxid Redox Signaling.* 2017;26(17):986–99. DOI: [10.1089/ars.2016.6820](https://doi.org/10.1089/ars.2016.6820). PMID: 27411305; PMCID: [PMC5467121](https://pubmed.ncbi.nlm.nih.gov/PMC5467121/)
- Wink DA, Vodovotz Y, Cook JA, Krishna MC, Kim S, Coffin D, et al. The role of nitric oxide chemistry in cancer treatment. *Biochemistry.* 1998;63(7):802–9. PMID: 9721332
- Fukumura D, Kashiwagi S, Jain RK. The role of nitric oxide in tumour progression. *Nat Rev Cancer.* 2006;6(7):521–34. DOI: [10.1038/nrc1910](https://doi.org/10.1038/nrc1910). PMID: 16794635
- Graziewicz M, Wink DA, Laval F. Nitric oxide inhibits DNA ligase activity: potential mechanisms for NO-mediated DNA damage. *Carcinogenesis.* 1996;17(11):2501–5. DOI: [10.1093/carcin/17.11.2501](https://doi.org/10.1093/carcin/17.11.2501). PMID: 8968069
- Lala PK, Chakraborty C. Role of nitric oxide in carcinogenesis and tumour progression. *Lancet Oncol.* 2001;2(3):149–56. DOI: [10.1016/S1470-2045\(00\)00256-4](https://doi.org/10.1016/S1470-2045(00)00256-4). PMID: 11902565
- Hu Ya, Xiang J, Su L, Tang Xi. The regulation of nitric oxide in tumor progression and therapy. *J Int Med Res.* 2020;48(2):300060520905985. DOI: [10.1177/0300060520905985](https://doi.org/10.1177/0300060520905985). PMID: 32090657; PMCID: [PMC7110915](https://pubmed.ncbi.nlm.nih.gov/PMC7110915/)
- Eyler CE, Wu Q, Yan K, MacSwords JM, Chandler-Militello D, Misuraca KL, et al. Glioma stem cell proliferation and tumor growth are promoted by nitric oxide synthase-2. *Cell.* 2011;146(1):53–66. DOI: [10.1016/j.cell.2011.06.006](https://doi.org/10.1016/j.cell.2011.06.006). PMID: 21729780; PMCID: [PMC3144745](https://pubmed.ncbi.nlm.nih.gov/PMC3144745/)
- Sun J, Steenbergen C, Murphy E. S-nitrosylation: NO-related redox signaling to protect against oxidative stress. *Antioxid Redox Signaling.* 2006;8(9–10):1693–705. DOI: [10.1089/ars.2006.8.1693](https://doi.org/10.1089/ars.2006.8.1693). PMID: 16987022; PMCID: [PMC2443861](https://pubmed.ncbi.nlm.nih.gov/PMC2443861/)
- Kruglyakov D, Ojha SK, Kartawy M, Tripathi MK, Hamoudi W, Bazbaz W, et al. Nitric oxide synthase inhibition prevents cell proliferation in glioblastoma. *J Mol Neurosci.* 2023;73(11):875–83. DOI: [10.1007/s12031-023-02166-3](https://doi.org/10.1007/s12031-023-02166-3). PMID: 37843719
- Iturriz-Rodríguez N, Sampron N, Matheu A. Current advances in temozolomide encapsulation for the enhancement of glioblastoma treatment. *Theranostics.* 2023;13(9):2734–56. DOI: [10.7150/thno.82005](https://doi.org/10.7150/thno.82005). PMID: 37284445; PMCID: [PMC10240814](https://pubmed.ncbi.nlm.nih.gov/PMC10240814/)
- Tanriover N, Ulu MO, Isler C, Durak H, Oz B, Uzan M, et al. Neuronal nitric oxide synthase expression in glial tumors: correlation with malignancy and tumor proliferation. *Neurol Res.* 2008;30(9):940–4. DOI: [10.1179/174313208X319099](https://doi.org/10.1179/174313208X319099). PMID: 18671896
- Broholm H, Rubin I, Kruse A, Braendstrup O, Schmidt K, Skriver EB, et al. Nitric oxide synthase expression and enzymatic activity in human brain tumors. *Clin Neuropathol.* 2003;22(6):273–81. PMID: 14672505
- Fahey JM, Stancill JS, Smith BC, Girotti AW. Nitric oxide antagonism to glioblastoma photodynamic therapy and mitigation thereof by BET bromodomain inhibitor JQ1. *J Biol Chem.* 2018;293(14):5345–59. DOI: [10.1074/jbc.RA117.000443](https://doi.org/10.1074/jbc.RA117.000443). PMID: 29440272; PMCID: [PMC5892570](https://pubmed.ncbi.nlm.nih.gov/PMC5892570/)



50. Girotti AW, Fahey JM, Korytowski W. Negative effects of tumor cell nitric oxide on anti-glioblastoma photodynamic therapy. *J Cancer Metastasis Treat.* 2020;6:52. DOI: [10.20517/2394-4722.2020.107](https://doi.org/10.20517/2394-4722.2020.107). PMID: 33564720; PMCID: [PMC7869587](https://pubmed.ncbi.nlm.nih.gov/PMC7869587/)
51. Scholzen T, Gerdes J. The Ki-67 protein: from the known and the unknown. *J Cell Physiol.* 2000;182(3):311–22. DOI: [10.1002/\(SICI\)1097-4652\(200003\)182:3\(311::AID-JCP1\)3.0.CO;2-9](https://doi.org/10.1002/(SICI)1097-4652(200003)182:3<311::AID-JCP1>3.0.CO;2-9). PMID: 10653597
52. Li LT, Jiang G, Chen Q, Zheng JN. Ki67 is a promising molecular target in the diagnosis of cancer (review). *Mol Med Rep.* 2015;11(3):1566–72. DOI: [10.3892/mmr.2014.2914](https://doi.org/10.3892/mmr.2014.2914). PMID: 25384676
53. Arandjelovic S, Ravichandran KS. Phagocytosis of apoptotic cells in homeostasis. *Nat Immunol.* 2015;16(9):907–17. DOI: [10.1038/ni.3253](https://doi.org/10.1038/ni.3253). PMID: 26287597; PMCID: [PMC4826466](https://pubmed.ncbi.nlm.nih.gov/PMC4826466/)
54. Elmore S. Apoptosis: a review of programmed cell death. *Toxicol Pathol.* 2007;35(4):495–516. DOI: [10.1080/01926230701320337](https://doi.org/10.1080/01926230701320337). PMID: 17562483; PMCID: [PMC2117903](https://pubmed.ncbi.nlm.nih.gov/PMC2117903/)
55. King K, Cidlowski J. Cell cycle regulation and apoptosis. *Annu Rev Physiol.* 1998;60(1):601–17. DOI: [10.1146/annurev.physiol.60.1.601](https://doi.org/10.1146/annurev.physiol.60.1.601). PMID: 9558478
56. Singh R, Letai A, Sarosiek K. Regulation of apoptosis in health and disease: the balancing act of BCL-2 family proteins. *Nat Rev Mol Cell Biol.* 2019;20(3):175–93. DOI: [10.1038/s41580-018-0089-8](https://doi.org/10.1038/s41580-018-0089-8). PMID: 30655609; PMCID: [PMC7325303](https://pubmed.ncbi.nlm.nih.gov/PMC7325303/)
57. De Zio D, Cianfanelli V, Cecconi F. New insights into the link between DNA damage and apoptosis. *Antioxid Redox Signal.* 2013;19(6):559–71. DOI: [10.1089/ars.2012.4938](https://doi.org/10.1089/ars.2012.4938). PMID: 23025416; PMCID: [PMC3717195](https://pubmed.ncbi.nlm.nih.gov/PMC3717195/)
58. Resende FFB, Titze-de-Almeida SS, Titze-de-Almeida R. Function of neuronal nitric oxide synthase enzyme in temozolomide-induced damage of astrocytic tumor cells. *Oncol Lett.* 2018;15(4):4891–9. DOI: [10.3892/ol.2018.7917](https://doi.org/10.3892/ol.2018.7917). PMID: 29552127; PMCID: [PMC5840643](https://pubmed.ncbi.nlm.nih.gov/PMC5840643/)
59. Bandoorkwala M, Sengupta P. 3-Nitrotyrosine: a versatile oxidative stress biomarker for major neurodegenerative diseases. *Int J Neurosci.* 2020;130(10):1047–62. DOI: [10.1080/00207454.2020.1713776](https://doi.org/10.1080/00207454.2020.1713776). PMID: 31914343
60. Strobel H, Baisch T, Fitzel R, Schilberg K, Siegelin MD, Karpel-Massler G, et al. Temozolomide and other alkylating agents in glioblastoma therapy. *Biomedicines.* 2019;7(3):69. DOI: [10.3390/biomedicines7030069](https://doi.org/10.3390/biomedicines7030069). PMID: 31505812; PMCID: [PMC6783999](https://pubmed.ncbi.nlm.nih.gov/PMC6783999/)
61. Arora A, Somasundaram K. Glioblastoma vs temozolomide: can the red queen race be won? *Cancer Biol Ther.* 2019;20(8):1083–90. DOI: [10.1080/15384047.2019.1599662](https://doi.org/10.1080/15384047.2019.1599662). PMID: 31068075; PMCID: [PMC6606031](https://pubmed.ncbi.nlm.nih.gov/PMC6606031/)

Publisher's note: Genomic Press maintains a position of impartiality and neutrality regarding territorial assertions represented in published materials and affiliations of institutional nature. As such, we will use the affiliations provided by the authors, without editing them. Such use simply reflects what the authors submitted to us and it does not indicate that Genomic Press supports any type of territorial assertions.



Open Access. This article is licensed under the Creative Commons Attribution-NonCommercial-NoDerivatives 4.0 International License (CC BY-NC-ND 4.0). The license mandates: (1) Attribution: Credit must be given to the original work, with a link to the license and notification of any changes. The acknowledgment should not imply licensor endorsement. (2) NonCommercial: The material cannot be used for commercial purposes. (3) NoDerivatives: Modified versions of the work cannot be distributed. (4) No additional legal or technological restrictions may be applied beyond those stipulated in the license. Public domain materials or those covered by statutory exceptions are exempt from these terms. This license does not cover all potential rights, such as publicity or privacy rights, which may restrict material use. Third-party content in this article falls under the article's Creative Commons license unless otherwise stated. If use exceeds the license scope or statutory regulation, permission must be obtained from the copyright holder. For complete license details, visit <https://creativecommons.org/licenses/by-nc-nd/4.0/>. The license is provided without warranties.